

The LEGUE disk target selection for the LAMOST pilot survey

Li Chen¹, Jinliang Hou¹, Jincheng Yu¹, Chao Liu², Licai Deng², Heidi Jo Newberg³, Jeffrey Carlin³, Fan Yang², Yueyang Zhang², Shiyin Shen¹, Haotong Zhang², Jianjun Chen², Yuqing Chen², Norbert Christlieb⁴, Zhanwen Han⁵, Hsu-Tai Lee⁶, Xiaowei Liu⁷, Kaike Pan⁸, Jianrong Shi², Hongchi Wang⁹ and Zi Zhu¹⁰

- ¹ Key Laboratory for Research in Galaxies and Cosmology, Shanghai Astronomical Observatory, CAS, 80 Nandan Road, Shanghai, 200030, China chenli@shao.ac.cn; houlj@shao.ac.cn
- ² Key Lab for Optical Astronomy, National Astronomical Observatories, Chinese Academy of Sciences (NAOC)
- ³ Department of Physics, Applied Physics and Astronomy, Rensselaer Polytechnic Institute, 110 8th Street, Troy, NY 12180, USA
- ⁴ Center for Astronomy, University of Heidelberg, Landessternwarte, Königstuhl 12, D-69117 Heidelberg, Germany
- ⁵ Yunnan Astronomical Observatory, Chinese Academy of Sciences, Kunming 650011, China
- ⁶ Academia Sinica Institute of Astronomy and Astrophysics, Taipei, China
- ⁷ Department of Astronomy & Kavli Institute of Astronomy and Astrophysics, Peking University, Beijing 100875, China
- ⁸ Apache Point Observatory, PO Box 59, Sunspot, NM 88349, USA.
- ⁹ Purple Mountain Observatory, Chinese Academy of Sciences, Nanjing 210008, China
- ¹⁰ School of Astronomy and Space Science, Nanjing University, Nanjing 210008, China

Abstract We describe the target selection algorithm for the low latitude disk portion of the LAMOST Pilot Survey, which aims to test systems in preparation for the LAMOST spectroscopic survey. We use the PPMXL (Roeser et al. 2010) astrometric catalog, which provides positions, proper motions, B/R/I magnitudes (mostly) from USNO-B (Monet et al. 2003) and J/H/Ks from The Two Micron All Sky Survey (2MASS, see Skrutskie et al. 2006) as well. We chose 8 plates along the Galactic plane, in the region $0^\circ < \alpha < 67^\circ$ and $42^\circ < \delta < 59^\circ$, that cover 22 known open clusters with a range of ages. Adjacent plates may have small overlapping. Each plate covers an area 2.5° in radius, with central star (for Shark-Hartmann guider) brighter than 8th magnitude. For each plate, we create an input catalog in the magnitude range $11.3 < I_{mag} < 16.3$ and B_{mag} available from PPMXL. The stars are selected to satisfy the requirements of the fiber positioning system and have a uniform distribution in the I vs. $B - I$ color-magnitude diagram. Our final input catalog consists of 12,000 objects on each of 8 plates that are observable during the winter observing season in Xinglong Station of the National Astronomical Observatory of China.

Key words: disk; Milky Way; stars; spectroscopy; survey; pilot

1 INTRODUCTION

The Guo Shou Jing Telescope (GSJT, formerly the Large Area Multi-fiber Spectroscopic Telescope - LAMOST) is a 4 meter telescope with 4000 fibers in the focal plane (Cui et al. 2012). The telescope is

located at Xinglong Station, located 114 km to the east north east (ENE) of Beijing and operated by the National Astronomical Observatories of China. Currently, a pilot survey is running on the telescope, in preparation for a full spectroscopic survey, which is expected to begin in late 2012. The survey has the potential to significantly increase our understanding on the substructures of the Galactic stellar spheroid and different disk components through measurements of radial velocities, metallicities and effective temperatures for millions of stars (Deng et al. 2012).

We describe here a latitude disk survey concentrated on open clusters, that is being conducted as part of the LAMOST Pilot Survey. The pilot survey mainly aims to test the LAMOST system, in preparation for coming main survey. The pilot survey targets fainter objects on dark nights (Yang et al. 2012, Carlin et al. 2012), and brighter objects when the moon is bright or the atmosphere has low transparency (Zhang et al. 2012). The footprint of the bright night disk survey is shown in Figure 1 overlaid on a starcount map from SDSS photometry. The magenta part is the disk survey region centered at $b=0^\circ$ which will be discussed in this paper.

One of the primary science objectives of the LAMOST disk survey is to investigate the structure of the thin/thick disks of the Galaxy, including the chemical abundance as a function of position within the disk and the extinction in the disk. In the main survey, we expect to cover 300 open clusters in the low Galactic latitude region, and obtain stellar radial velocities as well as abundance information for stars as faint as $r = 16^m$ in the cluster fields. This will be the largest spectroscopic data sets for studying the properties of Galactic open clusters, including the structure, dynamics, and evolution of the disk as probed by open clusters (Chen et al. 2003; Ahumada et al. 2011).

Some of the expected scientific outputs from the disk pilot survey include:

- significant improvements in essential parameter measurement of the targeted open clusters, using kinematic membership information and homogeneous abundance data.
- a database of spectroscopically confirmed cluster members in the outer parts of the clusters, that will provide good targets for detecting or verifying possible tidal tails of these stellar clusters.
- a large sample of young stellar objects across the surveyed area, which will provide important clues to studies of large-scale star formation and the history of Galactic star formation as well as information of the 3D extinction in the Galactic plane.
- tens of thousands of spectra of bright disk stars that can be used to characterize the chemistry and kinematics of the thin disk.

The open clusters are particularly important to the survey, since some of the well characterized open clusters provide important “standards” for a range of stellar types that can be used to calibrate the LAMOST observations and data-processing pipeline.

In section 2, we describe the footprint of the survey as well as the catalog from which the targets were selected. In section 3, we describe the selection of spectroscopic targets, including selection in color and magnitude, the effects of blending in a crowded field, and the properties of the selected spectroscopic targets. Finally, we summarize the paper.

2 FOOTPRINT AND INPUT CATALOG

For the disk pilot survey, we have chosen 8 plates along the Galactic plane that are nearly uniformly distributed in Galactic longitude, and in a range of right ascension and declination that will make them easily observable with GSJT. Telescope design favors observations with $-10^\circ < \delta < 60^\circ$; lower declinations are unobservable, and the effective aperture and image quality of the telescope decreases rapidly at declinations above $\delta = 60^\circ$. Since the observations should be taken near the meridian, it is important to spread the target fields out in Galactic longitude so that there are targets available at all right ascensions. The part of the sky observed is $0^\circ < \alpha < 67^\circ$, and $42^\circ < \delta < 59^\circ$. Adjacent plates may overlap slightly. Each plate covers a circle area of a radius 2.5° , with central star (for the Shack-Hartmann guider) brighter than $V = 8^m$. It is a requirement that each field observed by LAMOST have a bright star in the center so that the figure of the mirrors can be actively adjusted to focus stellar images in the focal plane.

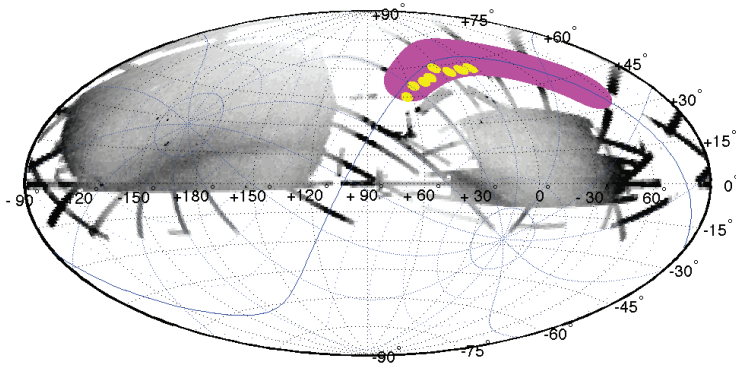


Fig. 1 The footprint of the bright night disk survey in equatorial coordinates overlaid on a starcount map from SDSS photometry. The magenta disk survey region is centered on the Galactic plane and the yellow circular areas are eight plates that were chosen for the pilot survey .

We were able to select fields that cover 22 previously identified star clusters. Table 1 shows the selected open clusters within coverage of the designed disk pilot survey plates. The angular distance between the cluster center and the plate center is less than 2 degrees in all cases. We also list here the parameters (Dias et al. 2002; WEBDA) for each cluster, including (if available) cluster name, the position, reddening and distance, the average proper motion and radial velocity, the cluster age estimation and the corresponding number of the survey plate. Some of the clusters have been poorly studied and we expect to obtain their kinematic and chemical information for the first time from the pilot survey database.

Individual stellar targets are selected from the PPMXL astrometric catalog (Roeser et al. 2010), which includes positions, proper motions, rough BRI magnitudes, and JHK magnitudes from 2MASS. PPMXL is a full sky catalog of positions, proper motions, 2MASS and optical photometry of 900 million stars and galaxies, aiming to be complete for the brightest stars down to about $V = 20^m$. It is the result of a re-reduction of USNO-B1 observations, supplemented with 2MASS and ICRS results. PPMXL is currently the largest collection of ICRS proper motions with typical errors ranging from 4 mas yr^{-1} to more than 10 mas yr^{-1} , depending on the object’s observational history.

In PPMXL, the photometric information from USNO-B1.0 is listed, as well as the NIR photometry from 2MASS when available. The B, R, I magnitudes in the USNO B1.0 magnitude system are rather crude, and there are discrepancies in the magnitude system from field to field and from early to late epochs. However, PPMXL is the only source that provides photometry in optical bands for low galactic latitude targets, which is necessary as an input catalog for our disk pilot survey.

Figure 2 shows the star number density in one of our plate regions, centered at $(\alpha = 5.1421^\circ, \delta = 56.5569^\circ; l = 118.6619^\circ, b = -6.0655^\circ)$. The PPMXL catalog lists 2.2×10^5 point objects in this area. On average there are over 11 thousand targets per square degree in this low Galactic latitude region, complete in magnitude to $I \sim 16.3^m$.

3 TARGET SELECTION AND INPUT CATALOG DESIGN

3.1 Target Selection Process

For each of our selected plates, we must create an input catalog of about three times as many stars as can be observed, from which the fiber assignment software will select the actual targets. Since GSJT

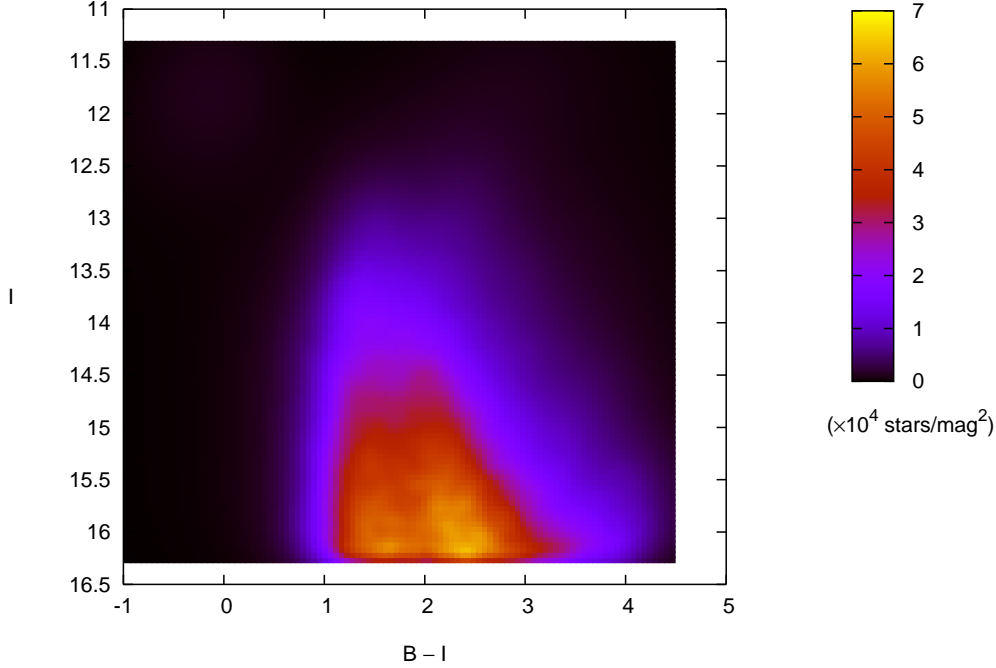


Fig. 2 The star number density (in unit of 10^4 stars/mag^2) in one of our plate region centered at ($RA = 5.1421^\circ$, $DEC = 56.5569^\circ$), using PPMXL as the input catalog, includes total of 2.2×10^5 targets. Color bar on the right showing different number density scales.

contains 200 fibers per square degree in the focal plane, we select $600 \text{ stars deg}^{-2}$ in the input catalog. We explain here how we select stars with $11.3 < I_{\text{mag}} < 16.3$ and available B_{mag} from PPMXL. Additionally, targets are selected to favor open cluster members, satisfy the requirements of the fiber positioning system, and maintain a uniform distribution in I, B-I color-magnitude space.

We developed our target selection algorithm following the scheme below:

- For every LAMOST survey field, we begin with input catalogs of a bright subset with $11.3 < I_{\text{mag}} < 14.3$ and a faint subset with $14.3 < I_{\text{mag}} < 16.3$. Objects are then extracted from PPMXL catalog.
- To prevent contamination of spectra by nearby stars (the blending effect, see discussion in the next section), we eliminate all stars that have a similar brightness or brighter neighbor within $5''$. Note that the LAMOST fiber diameter is $3.3''$ and the typical seeing in Xinglong station is around $2''$ to $3''$.
- To prevent local over density for fiber allocation, we set $6''$ as the minimum spatial distance for all selected stars in the following steps.
- We eliminate very high proper motion objects; the proper motion limit is $PM < 100 \text{ mas yr}^{-1}$. Note that the typical mean observation epochs for PPMXL sources are around 1970's or 1980's.
- Assigning highest priority to cluster members, whenever membership information is available in Kharchenko's catalog (Kharchenko et al. 2005), which is estimated based on the proper motion of individual stars in the cluster region.

- For the remainder of the targets, we perform uniformly sampling in color-magnitude space (B-I vs.I) by randomly selecting stars on the color-magnitude diagram (CMD). For instance, for the bright subset of Plate 1 we set the magnitude range as $11.3^m < I < 14.3^m$ and color term range $-1.5^m < (B - I) < 4.5^m$ which consisting totally about 36000 stars. First we generate a random point in the $(B - I) \sim I$ space, then within a search radius of 0.03 mag (roughly the average distance on the color-magnitude space) select the object closest to the random point as our sample star. Meanwhile, all the selected stars will satisfy the spatial distance limit of 6". The iteration ends up with a bright sub-catalog of 12000 stars ready for the fiber assignment software to select the actual targets. Here we note that the magnitude from PPMXL is rather crude.

It was intended that the bright and faint dataset sent to fiber assignment separately, and two pointings (one brighter and one fainter) would be done at each position. Instead, the two lists were merged before fiber assignment for the pilot survey, and in some cases a second or third pointing was constructed (with many repeated sources).

3.2 Blending in a crowded field

For a fiber fed multiobject spectroscopic telescope, e.g. GSJT, blending, which can be defined as at least two objects are captured by a fiber in an exposure, must be taken into account when the telescope targets crowded fields, e.g. the Galactic disk, open clusters and etc.

LAMOST contains 4000 fibers on the 1.75-meter-diameter focal plane; each fiber has an aperture of 3.3 arcsec. When a fiber is targeting an object, some flux contributed by its neighboring objects may also be recorded. Hence, the final processed spectra could be very strange if it is contaminated by the blending objects. In order to investigate the probability of the blending in LEGUE disk survey, we make a simple simulation.

We assume that 1) all objects in the simulation are point sources; 2) the range of the brightness of the objects covers $10 < m < 18$ mag, the fainter objects are ignored; 3) we only “observe” objects brighter than 16 mag, the objects between 16 and 18 mag only contribute to the blending; 4) the luminosity function is studied using SDSS photometry catalog and it can be approximately fitted by $A(m) \sim \exp(0.5m)$; and 5) the PSF is a Gaussian, in which the σ is smaller than the dome seeing by a factor of 2.35.

In the simulation we consider a circular, one square degree region filled with uniformly distributed objects (down to 18 mag). The density is from 2,500 to 25,000 stars/square degree, which is the typical density range in the outer disk and open clusters. Then we assign fibers for all objects with $m < 16$ mag given the dome seeing. For each fiber we calculate the ratio of the total flux from the neighboring objects (only those located within $3 \times \text{seeing}$ are considered) to that from the target in the fiber aperture. If the ratio is higher than 10%, we mark this fiber as an significant blended fiber. Note that the sky flux are ignored in the calculation. The fraction of the significant blended fibers in the field is defined as the probability of the blending.

We did the simulation for the seeing of 2", 3" and 4". The results are shown in Figure 3. We find that the probability of more than 10% flux of the blending objects being in the fiber aperture increases linearly with the density of the objects. Moreover, the bigger the seeing the higher the probability of the seeing. For instance, at a center region of an open cluster, in which the density can be around 10,000 per square degree, the LAMOST spectra will suffer about 0.7% significant blending, in each plate given the seeing of 2". It increases to 1% and 1.3% when the seeing is up to 3" and 4", respectively. It is worthy to note that in practice even fainter neighboring objects, e.g. objects with strong emission lines, out skirt of a neighboring galaxy, nearby emission nebulae etc., may also contribute to the flux. This limit will constrain the target selection for the disk survey to either avoid the very crowded region or accept the fact that there would be a few percent blended spectra and later develop a pipeline to deal with it.

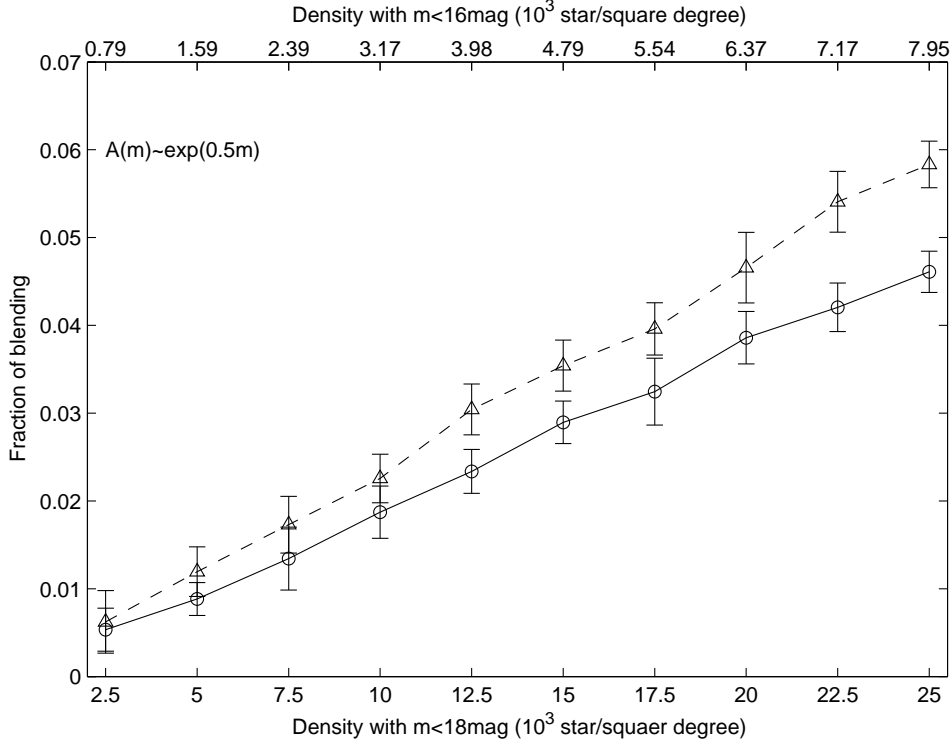


Fig. 3 The simulation of the blending within a fiber aperture. The X-axis on bottom is the density of the simulated objects with $m < 18$ mag, while on top is the density of the objects with $m < 16$ mag corresponding to the bottom X-axis. The luminosity function is assumed as $A(m) \sim \exp(0.5m)$, which is approximately estimated from SDSS photometry. The dotted, dashed, solid lines with triangles, rectangles and circles show the probability of more than 10% flux of the blending objects being in the fiber aperture when fibers are assigned to all objects with $m < 16$ mag given the dome seeing being 2, 3, and 4 arcsec, respectively. The error is estimated from a Monte Carlo approach.

3.3 Sample Plate for the Disk Portion of the Pilot Survey

As an example of the outputs from the target selection process, Figure 4 shows the color-magnitude distribution of selected targets as a bright subset (left panel) ($11.5 < I_{\text{mag}} < 14.3$) for Plate 1 and the spatial distribution (right panel) of selected stars. It can be seen that our uniform selection in color-magnitude space favors bluer as well as brighter objects in the input catalog. There are two open clusters well within the field of view of Plate 1 (centered at $\text{RA}=5.1421^\circ$, $\text{DEC}=56.5569^\circ$): ASCC 2 and ASCC 3. We assign highest priority to members (87 stars) of these clusters (membership information from Kharchenko et al. 2005). Here the output of our selection algorithm largely achieved the basic goal for target selection from field disk stars: we would like to sample a larger fraction of the rarer stars than the less rare, and a larger fraction of the interesting than the less interesting.

In this plate, we expect to observe all 87 open cluster member stars which can be used to calibrate the spectra quality and stellar parameters, especially the radial velocity and metallicity.

Figure 5 shows the color-magnitude distribution of targets in a faint subset (left panel) ($14.3 < I_{\text{mag}} < 16.3$) and the corresponding spatial distribution (right panel) of selected stars. Since the mag-

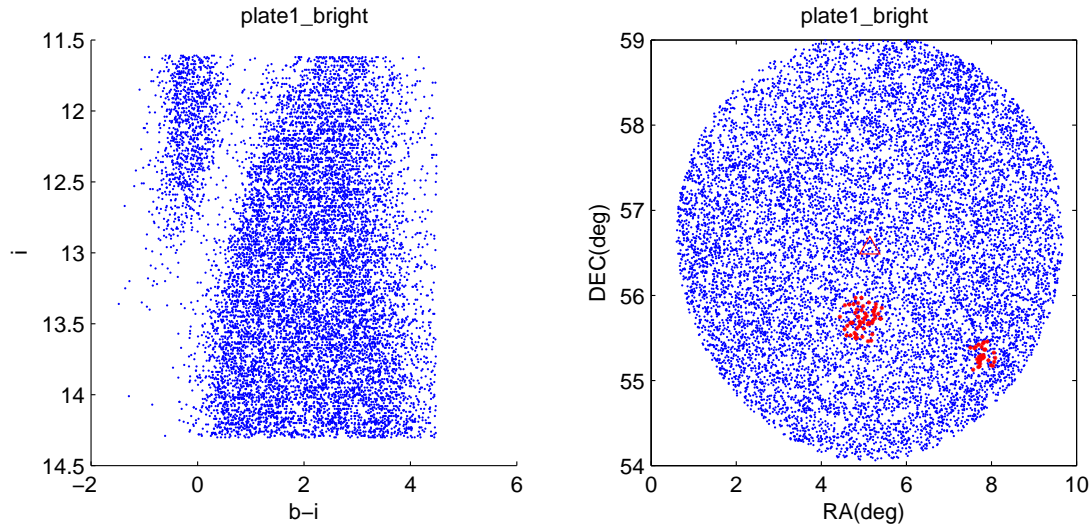


Fig. 4 Left: the color-magnitude distribution of selected targets as a bright subset ($11.3 < I_{\text{mag}} < 14.3$) for plate1, satisfying requirement for SSS fiber-assignment; right: spatial distribution of selected stars. Red *: OC members, red triangle: plate center

nitude limit in Kharchenko’s catalog (Kharchenko et al. 2005) is brighter than $V \sim 14^m$, there are no membership information available for this faint subset. In the future, we will use astrometric catalogs (e.g. PPMXL and UCAC3) to determine cluster membership to a deeper magnitude limit from proper motion.

4 SUMMARY

We have described the target selection algorithm for eight low latitude, bright plates that are planned to be observed during the LAMOST Pilot Survey. Stars from 22 open clusters will be observed on these plates. To date, 5 plates have been observed successfully, and the data reductions and quality assessment is being conducted. This portion of the Pilot Survey is in preparation for a larger survey that will cover 300 Galactic open clusters.

The highest priority targets on these plates are known or suspected members of Galactic open clusters. Other disk stars in the $11.3 < I_{\text{mag}} < 16.3$ range were selected uniformly over I, B-I color-magnitude phase space. Very high proper motion objects are not targeted. Positions, proper motions, and magnitudes are taken from the PPMXL catalog.

The spectra observed in this disk portion of the LAMOST Pilot Survey will be used for studies of Galactic open clusters, to investigate young stellar objects, and to study the chemistry and kinematics of disk stars. The open clusters stars will be important calibrators for the main spectroscopic survey.

Acknowledgements We thank the referee, Sanjib Sharma, for helpful comments on the manuscript. This work was funded by the National Natural Science Foundation of China (NSFC) under No. 11173044(PI:Hou), 11073038(PI:Chen), 10573022, 10973015, 11061120454 (PI:Deng), the Key Project No.10833005(PI:Hou), the Group Innovation Project No.11121062, and the US National Science Foundation (NSF) grant AST 09-37523. Chinese Academy of Science is acknowledged for providing a initial support by grant number GJHZ200812.

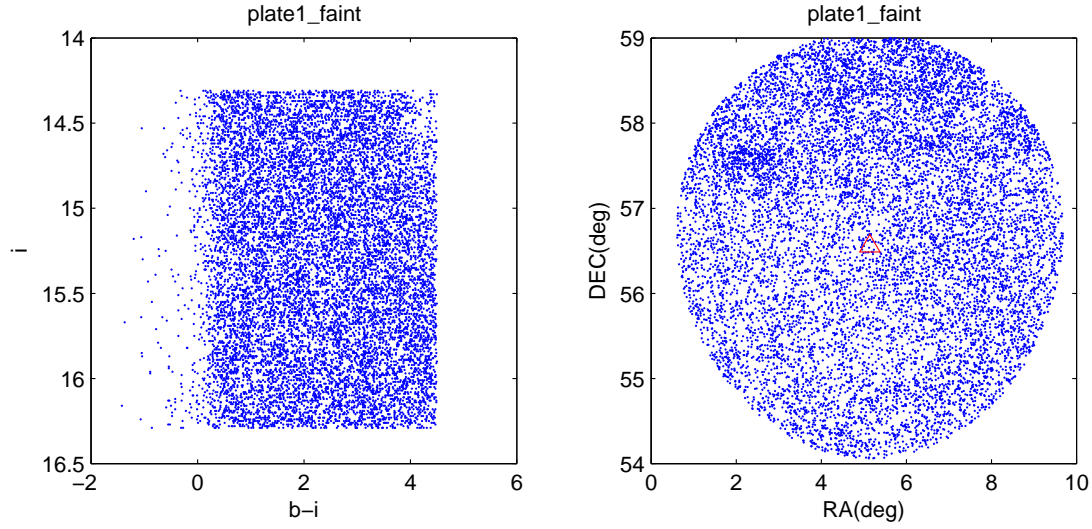


Fig. 5 Left: the color-magnitude distribution of selected targets as a faint subset ($14.3 < I_{\text{mag}} < 16.3$) for Plate-1, satisfying requirement for SSS fiber-assignment; right: spatial distribution of selected stars. Red triangle: plate center

Table 1 Properties of open clusters in the disk pilot survey area.

Name	RA h m s	Dec d m s	l ($^{\circ}$)	b ($^{\circ}$)	Ebv	Dist pc	$\mu_{\alpha \cos \delta}$ mas/yr	μ_{δ} mas/yr	R_v km/s	Age Gyr	Plate Nr.
ASCC 2	0 19 51.6	55 42 36	118.46	-6.89	0.10	1200	-0.91	-3.94		0.676	1
Stock 21	0 29 49.2	57 55 12	120.05	-4.83	0.40	1100	-0.12	-1.52		0.525	1
ASCC 3	0 31 8.4	55 16 48	120.02	-7.48	0.17	1700	-1.92	-1.25	-37.00	0.079	1
King 2	0 50 60.0	58 10 48	122.87	-4.69	0.31	5750				5.023	2
IC 1590	0 52 48.0	56 37 48	123.12	-6.24	0.32	2384	-1.36	-1.34	-37.50	0.007	2
ASCC 5	0 57 57.6	55 50 24	123.85	-7.02	0.25	1500	-3.10	-2.91	-43.00	0.011	2
NGC 657	1 43 20.9	55 50 24	130.22	-6.30							3
ASCC 6	1 47 13.2	57 43 48	130.34	-4.34	0.30	1200	-1.02	-1.18	-20.00	0.148	3
NGC 743	1 58 37.0	60 9 36	131.20	-1.63							4
ASCC 7	1 58 55.2	58 58 12	131.54	-2.77	0.50	2000	-0.57	-3.08	-49.00	0.023	4
Stock 2	2 14 24.0	59 16 12	133.36	-1.92	0.34	380	16.22	-13.39	-2.85	0.148	4
NGC 869	2 19 4.8	57 8 60	134.63	-3.72	0.48	2079	-0.49	-0.90	-39.82	0.019	4
Basel 10	2 19 28.1	58 17 60	134.30	-2.62	0.77	1944	1.47	0.35		0.041	4
ASCC 8	2 20 49.2	59 36 36	134.02	-1.33	0.55	2200	-1.24	0.57	-42.09	0.006	4
NGC 884	2 22 1.2	57 8 24	135.01	-3.60	0.56	2345	-0.84	-0.23	-38.14	0.013	4
Trumpler 2	2 36 54.0	55 55 12	137.37	-3.97	0.32	649	1.40	-5.57	-39.00	0.085	5
Czernik 12	2 39 12.0	54 55 12	138.08	-4.75							5
NGC 1220	3 11 40.1	53 20 24	143.04	-3.96	0.70	1800				0.060	6
King 5	3 14 36.0	52 43 12	143.74	-4.27		1900			-52.00	0.759	6
Czernik 15	3 23 12.0	52 15 0	145.10	-3.97							6
King 7	3 59 0.0	51 47 60	149.77	-1.02	1.25	2200				0.661	7
Berkeley 11	4 20 36.0	44 55 12	157.08	-3.64	0.95	2200	1.45	-2.37		0.110	8

References

- Ahumada, A. V., Bragaglia, A., Tosi, M. et al. 2011, *RevMexAA*, 40, 265
 Carlin, J. L., Lépine, S., Newberg, H. J., et al. 2012, *RAA*, in press

- Chen, L., Hou, J.L. & Wang, J.J. 2003, AJ, 125,1397
- Cui X. Q., Zhao, Y.H., Chu, Y.Q. et al. 2012, RAA, in press
- Deng, L., Newberg, H. J., Liu, C., et al. 2012, RAA, in press
- Dias, W.S., Alessi, B.S., Moitinho, A., et al. 2002, A&A, 389, 871
- Kharchenko, N. V., Piskunov, A. E., Roeder, S., et al. 2005, A&A, 438, 1163
- Monet D.G., Levine S.E., Casian B., et al. 2003, AJ, 125, 984
- Roeser S., Demleitner M., and Schilbach E. 2010, AJ, 139, 2440
- Skrutskie, M. F.; Cutri, R. M.; Stiening, R. et al. 2006, AJ, 131, 1163
- WEBDA: <http://www.univie.ac.at/webda/>
- Yang, F., Carlin, J. L., Liu, C. et al. 2012, RAA, in press
- Zhang, Y. Y., Carlin, J. L., Liu, C. et al. 2012, RAA, in press